Design of a Tracking Control System for an Optimal Post-Stall Manoeuvre Using Dynamic Inversion Approach

Pourtakdoust, S.H.*, Karimi, J., Shajiee, S. *****
Azad University, Science & Research Branch

* Professor, Department of Aerospace Eng., pourtak@sr.iau.ac.ir
** Graduate Research Assistant, jkarimi@ae.sharif.edu
*** Graduate Research Assistant, shajieesh@alum.sharif.edu

Key Words: *post stall - thrust vectoring control system [TVCS] - Herbst maneuver - dynamic inversion [DI] – optimal control*

Abstract

In this paper, a combination of optimal and non-linear control methodologies is utilized to perform an optimally determined Herbst type trajectory as a post stall maneuver for a typical fighter by means of Thrust Vectoring Control System [TVCS]. There are two major parts involved in this investigation. First, the Herbst maneuver is determined following a variational formulation of the problem over three major segments of the trajectory. Second, a closed-loop control system is designed for the aircraft by means of Dynamic Inversion (DI) method using a combination of aerodynamic control surfaces and TVCS. Results include time variations of optimal state trajectories and control strategies required for tracking with/without constraints.

1 Introduction

High maneuverability is one of the most important requirements for most fighter aircrafts. Post stall simulations have shown that high performance maneuvers in this region could cause tactical air superiority in close air combat situations and thus increase the maneuverability and agility of the aircraft. Fighters can often be designed to perform post stall maneuvers such as Herbst, using a combination of complicated control systems and new technology developments in the area of thrust vectoring [1]. Design of a complex three-dimensional post-stall trajectory is by itself a formidable task that can only be executed by advanced technology aircrafts equipped with thrust vectoring capabilities [1,2,3,4]. Fortunately, the optimal control theory provides a basis for determination of the optimized maneuver trajectory with/without constraints [5,6,7]. Determination of non-linear control systems for tracking complex super-maneuvers using different schemes such as DI method have been investigated by some researchers [8,9]. In this paper, the feasibility of performing the Herbst maneuver is investigated for a typical fighter aircraft where the desired optimal trajectory is obtained using variational formulation. In addition, a closed-loop tracking control system is designed for the selected aircraft by means of DI method using a combination of aerodynamic control surfaces and TVCS which satisfy the given physical constraints while tracking the desired optimal trajectory. Due to existing potential for thrust vectoring capability and related data, an F-18 HARV is selected for maneuver simulation.

2 Equations of Motion

Non-linear, six degrees of freedom governing equations of motion for a rigid aircraft assuming flat earth are presented in equation set (1) [9]:

$$\dot{v} = \frac{1}{m}\begin{bmatrix} -D + (Y + T_y)\sin(\beta) - mg\sin(\gamma) + \\ T_x\cos(\beta)\cos(\alpha) + T_x\cos(\beta)\sin(\alpha) \end{bmatrix}$$

$$\dot{\chi} = \frac{1}{mv\cos(\gamma)}\{L\sin(\mu) + (Y + T_y)\cos(\mu)\cos(\beta) + T_x[\sin(\mu)\sin(\alpha) - \cos(\mu)\sin(\beta)\cos(\alpha)] - T_z[\cos(\mu)\sin(\beta)\sin(\alpha) + \sin(\mu)\cos(\alpha)]\}$$

$$\dot{\gamma} = \frac{1}{mv}\{L\cos(\mu) - mg\cos(\gamma) - (Y + T_y)\sin(\mu)\cos(\beta) + T_x[\sin(\mu)\sin(\beta)\cos(\alpha) + \cos(\mu)\sin(\alpha)] + T_z[\sin(\mu)\sin(\beta)\sin(\alpha) - \cos(\mu)\cos(\alpha)]\}$$

$$\dot{\alpha} = q - \tan(\beta)[\tan(\alpha)p + \sin(\alpha)r)] + \frac{1}{mv\cos(\beta)} \times [-L + mg\cos(\gamma)\cos(\mu) - T_x\sin(\alpha) + T_z\cos(\alpha)]$$

$$\dot{\beta} = \sin(\alpha)p - \cos(\alpha)r + \frac{1}{mv}[mg\cos(\gamma)\sin(\mu) + (Y + T_y)\cos(\beta) - T_x\sin(\beta)\cos(\alpha) + T_z\sin(\beta)\sin(\alpha)]$$

$$\dot{\mu} = \frac{1}{\cos(\beta)} \times [\cos(\alpha)p + \sin(\alpha)r] - \frac{g}{v}\cos(\gamma)\cos(\mu)\tan(\beta) + \frac{L}{mv} \times [\tan(\gamma)\sin(\mu) + \tan(\beta)] + \frac{(Y + T_y)}{mv}\tan(\gamma)\cos(\mu)\cos(\beta) + \frac{T_x\sin(\alpha) - T_z\cos(\alpha)}{mv} \times [\tan(\gamma)\sin(\mu) + \tan(\beta)] - \frac{T_x\cos(\alpha) + T_z\sin(\alpha)}{mv} \times \tan(\gamma)\cos(\mu)\sin(\beta)$$

$$\dot{p} = \frac{1}{I_x I_z - I^2{}_{xz}}[I_z l(n + n_T) + I_{xz}(I_x - I_y + I_z)pq + (I_z(I_y - I_z) - I_{xz}{}^2)qr]$$

$$\ddot{q} = \frac{1}{I_y}[m + m_T + (I_z - I_x)pr + I_{xz}(r^2 - p^2)]$$

$$\dot{r} = \frac{1}{I_x I_z - I_{xz}^2}[I_{xz} l + I_x(n + n_T) + (I_x(I_x - I_y) + I_{xz}^2)pq - I_{xz}(I_x - I_y + I_z)qr]$$

$$\dot{x} = v\cos(\gamma)\cos(\chi)$$

$$\dot{y} = v\cos(\gamma)\sin(\chi)$$

$$\dot{h} = v\sin(\gamma) \qquad (1)$$

where $v, \alpha, \beta, \gamma, \chi, \mu$ are velocity, angle of attack, sideslip angle, flight path angle, heading angle about the velocity vector and the bank angle respectively. p, q, r are the angular rates in the body-axis roll, pitch and yaw; x, y, h are the components of aircraft 3-D position and T_x, T_y, T_z are the body axis components of thrust and m is the aircraft mass.

3 Optimal Trajectory Determination

3.1 Herbst Maneuver Description

Herbst maneuver is taken after Dr. Herbst's who first presented the idea of flight in post stall region. Dr. Herbst defined super maneuverability as the ability to perform a maneuver at high angle of attack with controlled sideslip angle. The X-31 aircraft performed this maneuver for the first time. When the maneuver begins, aircraft angle of attack increases until it enters the post stall region and the velocity decreases. Obviously in this situation, the aircraft cannot be controlled only by aerodynamic control surfaces. Therefore the TVCS should be applied in order to compensate for the lack of aerodynamic control effectiveness. Subsequently, aircraft performs a 180-degree turn, and accelerates in a new flight direction [1]. A three-dimensional view of the Herbst maneuver is shown in figure (1).

3.2 Optimal Control Problem Formation

The mathematical model, based on the equation set (1), is developed in order to obtain the optimal trajectory for the assumed post stall maneuver. Following methodologies and assumptions are applied in order to solve the proposed optimal control problem:

1) α , μ are considered as control variables.
2) β is ignored due to definition of the Herbst maneuver.
3) Because of low velocity and thus low dynamic pressure in the Herbst maneuver,

the aerodynamic control surfaces are not very effective. So they are kept at fixed positions in optimal control formulation.

4) Throttle setting is considered at its maximum value during the maneuver.
5) All of the aircraft aerodynamic derivatives are taken from reference [3]. Because of the non-linear nature of the problem, these derivatives are fitted with polynomials that are functions of angle of attack. For example, $CL_q = f(\alpha)$ is estimated with a second order polynomial.
6) T_x, T_y, T_z are defined as:

$$T_x = T\cos(\delta_{pv})\cos(\delta_{yv}),\ T_y = T\cos(\delta_{pv})\sin(\delta_{yv}),$$
$$T_z = T\sin(\delta_{pv}) \qquad (2)$$

where δ_{yv}, δ_{pv} are thrust vector angles providing yaw and pitch moments.

In the optimal control problem, the state vector is comprised of $\mathbf{X} = [v\ \gamma\ \chi\ p\ q\ r\ x\ y\ h]^T$ and the control vector includes $\mathbf{u} = [\alpha\ \mu\ \delta_{yv}\ \delta_{pv}]^T$. There are some constraints on the thrust vector angles, the rate of deflection of thrust vector angles and symmetric load-factor (n_Z) that must be satisfied [2,3,4]:

$$-25^\circ \le \delta_{pv} \le 16^\circ, -20^\circ \le \delta_{yv} \le 11^\circ \qquad (3)$$

$$\left|\dot{\delta}_{pv}\right| \le 80\frac{\text{deg}}{\text{sec}}, \left|\dot{\delta}_{yv}\right| \le 80\frac{\text{deg}}{s} \qquad (4)$$

$$-2 \le n_z = \frac{L\cos(\alpha) + D\sin(\alpha) - T_z}{mg} \le 4.3 \qquad (5)$$

The performance index (J) is considered as a terminal control criterion with free final time. Thus for this problem, the goal is to minimize the deviation of the system states from their desired value $\mathbf{r}(t_f)$ [5] .

$$J = h(\mathbf{X}(t_f), t_f) = \left\|\mathbf{X}(t_f) - \mathbf{r}(t_f)\right\|^2 \mathbf{K} \qquad (6)$$

where K is a weighting matrix in the performance index (J).

The necessary conditions for optimal trajectory and control are derived from the system Hamiltonian defined in equation set (7):

$$H(\mathbf{X},\mathbf{u},\mathbf{p},t) = p_v\dot{v} + p_\chi\dot{\chi} + p_\gamma\dot{\gamma} + p_p\dot{p} + p_q\dot{q} + p_r\dot{r} + p_x\dot{x} + p_y\dot{y} + p_h\dot{h} \qquad (7)$$

where H is Hamiltonian function and $p_v, p_\chi, p_\gamma\ p_p, p_q, p_r\ p_x, p_y, p_h$ are the Lagrangian coefficients. Subsequently, the state, costate and the optimality condition as well as the required boundary conditions are developed.

$$\dot{\mathbf{X}}^*(t) = \frac{\partial H(\mathbf{X}^*(t),\mathbf{u}^*(t),\mathbf{p}^*(t),t)}{\partial \mathbf{p}} \qquad (8)$$

$$\dot{\mathbf{p}}^*(t) = -\frac{\partial H(\mathbf{X}^*(t),\mathbf{u}^*(t),\mathbf{p}^*(t),t)}{\partial \mathbf{X}} \qquad (9)$$

$$\frac{\partial H(\mathbf{X}^*(t),\mathbf{u}^*(t),\mathbf{p}^*(t),t)}{\partial \mathbf{u}} = 0 \qquad (10)$$

$$\mathbf{X}^*(t_0) = \mathbf{X_0} \qquad (11)$$

$$\mathbf{p}^*(t_f) = \frac{\partial h(\mathbf{X}^*(t_f))}{\partial \mathbf{X}} = \mathbf{K}[\mathbf{X}^*(t_f) - \mathbf{r}(t_f)] \qquad (12)$$

$$H(\mathbf{X}^*,\mathbf{u}^*,\mathbf{p},t_f) - \dot{\mathbf{X}}(t_f)\mathbf{K}[\mathbf{r}(t_f) - \mathbf{X}(t_f)] = 0 \qquad (13)$$

In order to simplify solution of the formed free final time optimal control problem, time is normalized as:

$$t = t_f \cdot \varsigma, \qquad 0 \le \varsigma \le 1, \qquad \frac{dA}{d\varsigma} = t_f\frac{dA}{dt} \qquad (14)$$

where t_f is constant and A describes state and co-state variables.

Obviously the formed Two-Point Boundary Value Problem (TPBVP) [Eq.(8)&(9)] cannot be solved by analytical methods. So it should be solved by means of an appropriate numerical method. In this study, the steepest descent approach is utilized to solve the resulting optimal control problem. It is important to obtain appropriate responses for

optimal states and control that can satisfy all of the constraints mentioned in relations (3) to (5).

3.3 Solving Methodology and Results

As stated above, the steepest descent (SD) methodology is adapted here to solve the resulting optimal control problem. SD approach is especially useful for non-constrained optimal problems; so in order to satisfy the constraints of the problem and simplify the solution procedures, the following assumptions are used:

1) Final time is taken to be free, so initially there is no time restriction on the maneuver.
2) The maneuver is broken down into 3 stages of simpler maneuvers [10,11]. Continuity of stages at stage connection points are imposed as part of boundary specification.
3) Steepest descent method requires an initial guess for control variables [5]. This guess is chosen such that all of the constraints are satisfied.
4) At every stage of the maneuver, two of the nine states are selected to minimize their deviation from the desired value. In the first stage v, γ, in second stage v, χ and in the third stage v, χ are chosen for this purpose.

Initial values of the state vector for the first stage are taken as:

$$[v_1\ \gamma_1\ \chi_1\ p_1\ q_1\ r_1\ x_1\ y_1\ h_1] = [100\ 0\ 0\ 0\ 0\ 0\ 0\ 0\ 1000]$$

while initial values of the state vector for the second stage will be:

$$[v_1\ \chi_1\ \gamma_1\ p_1\ q_1\ r_1\ x_1\ y_1\ h_1] = [30\ \ -1.025\ 1.0471\ .033\ 0.7725\ \ -.6907\ 553.4036\ \ -80.0302\ 1324.4]$$

And finally, initial values of the state vector for the third stage will turn out to be:

$$[v_1\ \chi_1\ \gamma_1\ p_1\ q_1\ r_1\ x_1\ y_1\ h_1] = [32\ \ -2.6178\ \ -0.0593\ 0.3539\ 0.6829\ \ -2.6992\ 511.5101\ \ -144.514\ 1384.18]$$

where the velocity is in m/sec, angles are in radians and angular rates are in rad/sec. Time history of some of the optimal states and controls for the Herbst maneuver are shown in figures (2) to (9). It is seen that the assumed constraints in relations (3) to (5) are satisfied and the load factor variation during the maneuver is in the acceptable range. As a result, the optimal trajectory is admissible. A three-dimensional graph of the obtained optimal maneuver is also shown in figure (10).

4 Control System Design

4.1 Mathematical Model

Once the optimal trajectory of the Herbst maneuver based on the typical fighter aircraft requirements is obtained, designing a suitable control system to track this trajectory is of interest. Equation set (1) is used again here as the mathematical model. The required aerodynamic derivatives are obtained from reference [3] and our aerodynamic model utilizes this data set.

Thrust forces, in contrast with the optimal control problem, are formulated in a new way:

$$T_x = T, T_y = T\delta_y, T_z = T\delta_z \qquad (15)$$

where $|\delta_y|, |\delta_z| \le 1$. It is assumed that thrust vector doesn't produce rolling moment.

The example chosen aircraft, namely F-18 HARV, has two right and left stabilators, which together can produce pitch and yaw moments and thus stabilators play the roles of both the elevator and ailerons. Defining left-hand stabilator deflection as *del* and similarly right-hand stabilator deflection as *der*, with positive magnitude when turning down, the equivalent elevator and aileron deflections can be derived as:

$$\delta_e = \frac{del + der}{2}, da = \frac{del - der}{2} \qquad (16)$$

Total equivalent aileron angle (δ_a) is calculated by adding the aerodynamic contribution of aileron to the aerodynamic contribution of da.

In this case, state and control vectors are chosen as $\dot{\mathbf{X}} = [v, \chi, \gamma, \alpha, \beta, \mu, p, q, r, x, y, h]$ and $\mathbf{u} = [\delta_a, \delta_r, \delta_e, \delta_y, \delta_z]$, respectively.

4.2 Dynamic Inversion [DI] Method

This method is specially used to solve tracking non-linear control problems. Assume the system dynamics as:

$$\dot{\mathbf{x}} = f(\mathbf{x}) + G(\mathbf{x})\mathbf{u} \ , \mathbf{y} = k(\mathbf{x}) \qquad (17)$$

Where $\mathbf{x}$ is $n \times 1$ the state vector, $\mathbf{u}$ is $m \times 1$ the control vector and $f(\mathbf{x}), G(\mathbf{x}), k(\mathbf{x})$ are nonlinear matrices. A linear relation, similar to equation (18), can be achieved between inputs and interested outputs by differentiating the output equation:

$$\dot{\mathbf{y}} = h(\mathbf{x}) + c(\mathbf{x})\mathbf{u} \qquad (18)$$

If equation (18) is inversed and solved for $\mathbf{u}$;

$$\mathbf{u} = c(\mathbf{x})^{-1} \times [\dot{\mathbf{y}} - h(\mathbf{x})] \qquad (19)$$

Then by substituting the desired output ($\dot{\mathbf{y}}_{\mathbf{d}}$) for $\dot{\mathbf{y}}$, the value of control signal ($\mathbf{u}$) is calculated in order to obtain a suitable tracking of the desired outputs.

4.3 Closed-Loop Control System

In its most basic, first-order form, DI requires that the system has at least as many inputs as states. This is generally not the case for aircraft control systems. This problem is solved by formulating the problem as a two-time scale problem [9]. Thus with using a model reduction method, the fast dynamics corresponds to the states p, q, r and will be controlled by inputs $\delta_a, \delta_r, \delta_e, \delta_y, \delta_z$. The slow dynamics corresponds to the slow states α, β, μ and will be controlled by inputs p, q, r. The reason of using two-time scale is that the effect of the aerodynamic control surfaces and thrust vectoring controls on states α, β, μ, as slow dynamics, is weaker than states p, q, r, as fast dynamics. The designed closed-loop control system with inner and outer loops are shown in figure (18).

4.4 Inner Loop Control System design

In the inner loop, the fast dynamics control system is designed. Desired state dynamics of inner-loop control system are defined as:

$$\dot{p}_d = k_p(p_c - p), \dot{q}_d = k_q(q_c - q), \dot{r}_d = k_r(r_c - r) \qquad (20)$$

where p_c, q_c, r_c are obtained from outer loop and k_p, k_q, k_r are the inner-loop gains. $\dot{p}, \dot{q}, \dot{r}$ relations in equation set (1) can be converted to the form required by equation (18):

$$h(\mathbf{x}) = \begin{bmatrix} \dfrac{I_{xz}(I_x - I_y + I_z)pq + [I_z(I_y - I_z) - I_{xz}^2]qr}{I_x I_z - I_{xz}^2} \\ \dfrac{(I_z - I_x)pr + I_{xz}(r^2 - p^2)}{I_y} \\ \dfrac{[I_x(I_x - I_y) + I_{xz}^2]pq - I_{xz}(I_x - I_y + I_z)qr}{I_x I_z - I_{xz}^2} \end{bmatrix} \qquad (21)$$

$$c(\mathbf{x}) = \begin{bmatrix} \dfrac{I_z}{I_x I_z - I_{xz}^2} & 0 & \dfrac{I_{xz}}{I_x I_z - I_{xz}^2} \\ 0 & \dfrac{1}{I_y} & 0 \\ \dfrac{I_{xz}}{I_x I_z - I_{xz}^2} & 0 & \dfrac{I_x}{I_x I_z - I_{xz}^2} \end{bmatrix} \qquad (22)$$

$$\begin{bmatrix} \dot{p} \\ \dot{q} \\ \dot{r} \end{bmatrix} = h(\mathbf{x}) + c(\mathbf{x}) \begin{bmatrix} l \\ m + m_T \\ n + n_T \end{bmatrix} \qquad (23)$$

Figure (17) shows the configuration of the designed inner-loop. Inner loop has two blocks. In the first block, Aerodynamic and thrust moments are obtained as:

$$\begin{bmatrix} l \\ m + m_T \\ n + n_T \end{bmatrix} = c^{-1}(\mathbf{x}) \times \left(\begin{bmatrix} \dot{p}_d \\ \dot{q}_d \\ \dot{r}_d \end{bmatrix} - h(\mathbf{x}) \right) \qquad (24)$$

The relation between unknown variables $\delta_a, \delta_r, \delta_e, \delta_y, \delta_z$ and the obtained moments is presented below:

$$l = qSb(C_{l\beta}\beta + \frac{b}{2v}(C_{lp}p + C_{lr}r) + C_{l\delta a}\delta_a + C_{l\delta r}\delta_r)$$

$$m + m_T = qSC(C_{m0} + C_{m\alpha}\alpha + \frac{C}{2v}C_{mq}q + C_{m\delta e}\delta_e) + T\delta_z l_{xT}$$

$$n + n_T = qSb(C_{n\beta}\beta + \frac{b}{2v}(C_{np}p + C_{nr}r) + C_{n\delta a}\delta_a + C_{n\delta r}\delta_r) + T\delta_y l_{xT} \quad (25)$$

l_{xT} is the longitudinal distance between engine thrust and aircraft center of gravity (C.G.). In the second block, obtained moments $l, m + m_T, n + n_T$ are divided between five control variables $\delta_a, \delta_r, \delta_e, \delta_y, \delta_z$. This is done in an iterative manner, first by assuming $\delta_y = \delta_z = 0$ at the beginning and thus $\delta_a, \delta_r, \delta_e$ are obtained from the equation set (25). This strategy continues until all of the aerodynamic control surfaces are saturated, then they remain at their maximum values and Thrust control variables are activated; δ_z is activated when δ_e is saturated and δ_y is activated when δ_r is saturated. Constraints on aerodynamic control surfaces are presented below:

$$-24^\circ \le \delta_a \le 24^\circ, -30^\circ \le \delta_r \le 30^\circ, -24^\circ \le \delta_e \le 10^\circ \quad (26)$$

4.5 Outer Loop Control System design

Desired dynamics of the outer-loop is defined as:

$$\dot{\alpha}_d = k_\alpha(\alpha_c - \alpha), \dot{\beta}_d = k_\beta(\beta_c - \beta), \dot{\mu} = k_\mu(\mu_c - \mu) \quad (27)$$

where α_c, μ_c are achieved from optimal control problem. In addition, it is assumed that $\beta_c = 0$ because of the Herbst maneuver definition and k_α, k_β, k_μ are the outer-loop gains. As mentioned before, the effect of the aerodynamic control surfaces and thrust vectors on α, β, μ is ignored, in comparison with their effect on p, q, r. Hence, $h(\mathbf{x})$ and $c(\mathbf{x})$ can be obtained similar to the inner loop case. The corresponding relation between the inputs and the desired outputs for the outer loop is:

$$\begin{bmatrix} p_c \\ q_c \\ r_c \end{bmatrix} = c^{-1}(\mathbf{x}) \times (\begin{bmatrix} \dot{\alpha}_d \\ \dot{\beta}_d \\ \dot{\mu}_d \end{bmatrix} - h(\mathbf{x})) \quad (28)$$

5 Conclusions

In this paper, initially an optimal model of the Herbst maneuver is obtained for a selected aircraft. Then a control system is designed in order to track the desired states, determined from the optimal control problem. As mentioned, the thrust vectoring commands δ_y, δ_z are applied when aerodynamic controls δ_r, δ_e are saturated. But no substitution is assumed for the conditions that δ_a is saturated. Hence, in the closed-loop control system design procedure, both conditions of unconstrained aileron δ_a, as well as constrained aileron are investigated. In the unconstrained aileron situation, the proposed inner-loop gains are $k_p = k_q = k_r = 30\frac{rad}{\sec}$ and the proposed outer-loop gains are $k_\alpha = k_\beta = k_\mu = 7\frac{rad}{\sec}$ respectively. In the constrained aileron case, the proposed inner-loop gains are $k_p = k_q = k_r = 30\frac{rad}{\sec}$ and the proposed outer-loop gains are $k_\alpha = k_\beta = k_\mu = 5\frac{rad}{\sec}$ respectively. These gains are obtained in order to achieve admissible tracking error for the Herbst maneuver and acceptable thrust controls. It is concluded from the results that for the unconstrained problem, the desired values of α, β, μ are tracked with good precision and β does not exceed one degree during the whole maneuver. In contrast, in the δ_a constrained problem, α, β, μ are not within the desired

values. As a result, it is proposed to apply thrust-vectoring control in roll direction, in this case, in order to achieve a more precise tracking of the desired trajectory during the maneuver. Variations of the control inputs and states for both the unconstrained and the constrained aileron, δ_a, during the maneuver are shown in figures (2) to (15). In addition, variation of the load factor, n_Z, in both the unconstrained and the constrained aileron during the maneuver is shown in figure (16). It is seen that the load factor is within the admissible region of equation (5) for both cases.

Authors are currently looking into the design of a robust control system to perform the Herbst maneuver when atmospheric turbulence is present. The result of this complementary research will be published later.

References

[1] Alcorn, C.W., Croom, M. A., Francis, M.S. and Ross, H., "*The X-31 aircraft: advances in aircraft agility and performance*", Aerospace Set, vol. 32, pp. 327-413, 1996.

[2] Bowers, Albion H. and Pahle, Joseph W., "*Thrust vectoring on the NASA F-18 high alpha research vehicle*", November 1996.

[3] http://www.dfrc.nasa.gov/Resarch/HARV/kempel2.html.

[4] Johnson, Steven A.," *A simple dynamic engine model for use in real-time aircraft simulation with thrust vectoring*", 1990.

[5] Kirk, E. Donald, "*Optimal control theory an introduction*", Prentice Hall, Englewood cliffs New Jersey.

[6] Slotine, Jean-Jacques E., " *Applied Nonlinear Control*", Prentice Hall, Englewood cliffs New Jersey, 1991.

[7] Well, K.H., Faber, B. and Berger, E.," Optimization of tactical aircraft maneuvers utilizing high angles of attack", *J. Guidance*, vol. 5, No. 2, pp. 244-250, 1998.

[8] Reiner, J., Balas, J.G., Garrard, W.L., " Robost Dynamic Inversion for Control of Highly Maneuverable Aircraft", *Journal of Guidance, control, and dynamics*, vol.18, No.1, January-February, pp. 18-23, 1995.

[9] Snell, S. Antony, Enns, Dale F. And Garrard Jr., William L., "Nonlinear inversion flight control for a supermaneuverable aircraft", *Journal of Guidance, control, and dynamics*, vol.15, No.4, July-August, , pp.976-984, 1992.

[10] Bush, Andy and Smith, Leon, "*Air combat basics: the scissors maneuver*", http://www.simhq.com/_air/air_054a.html.

[11] Walker, John R., "*Air superiority operations*", Brassey's (UK), 1989.

Figures

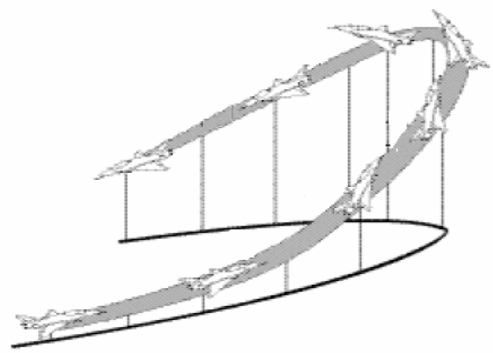

Fig. 1. A three-dimensional view of the Herbst maneuver structure

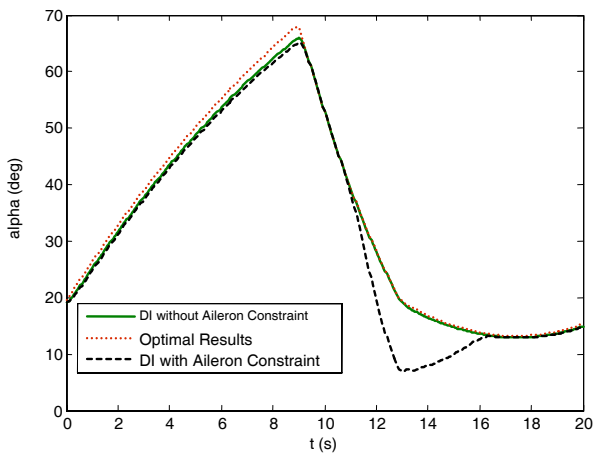

Fig. 2. Time variation of the angle of attack (deg)

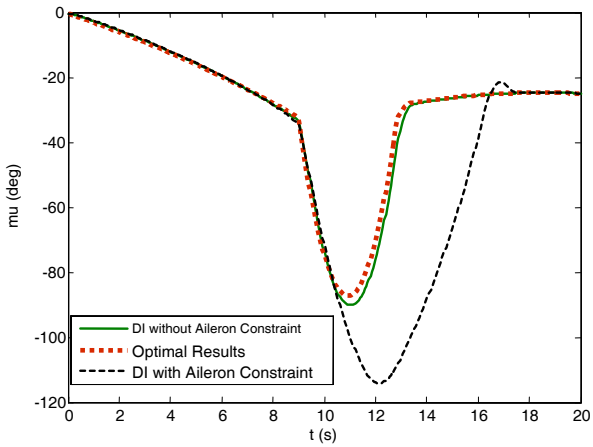

Fig. 3. Time variation of μ (deg)

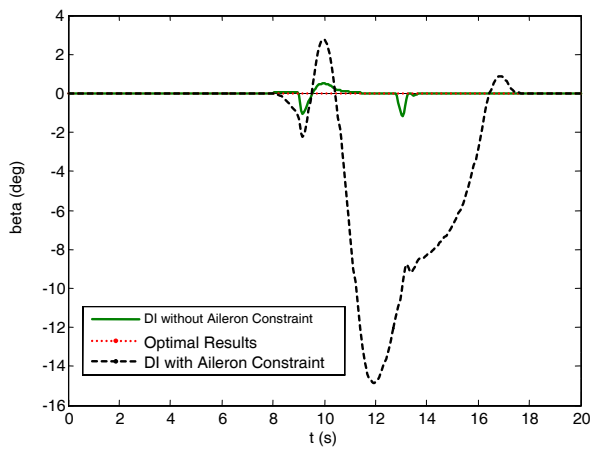

Fig. 4. Time variation of β (deg)

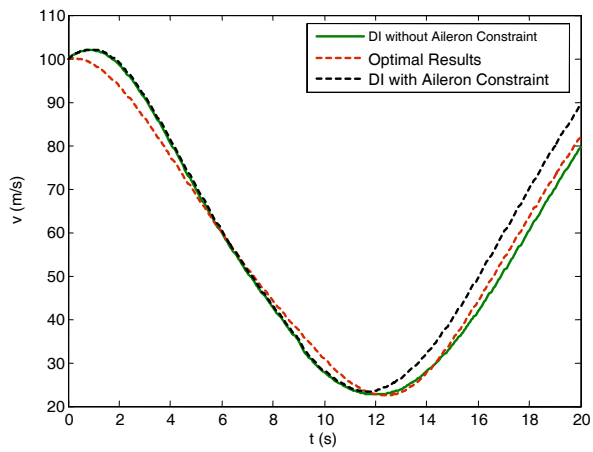

Fig. 5. Time variation of v (m/s)

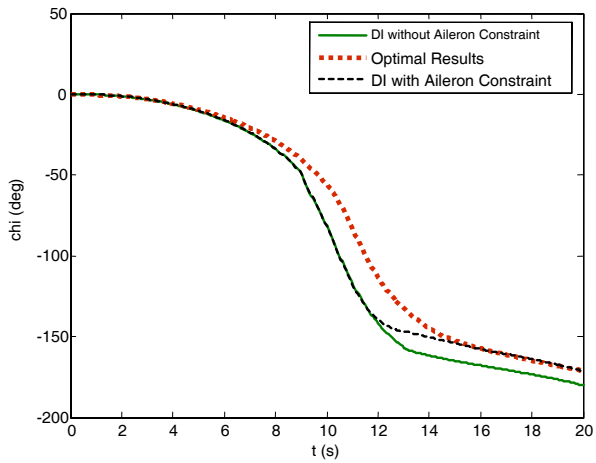

Fig. 6. Time variation of χ (deg)

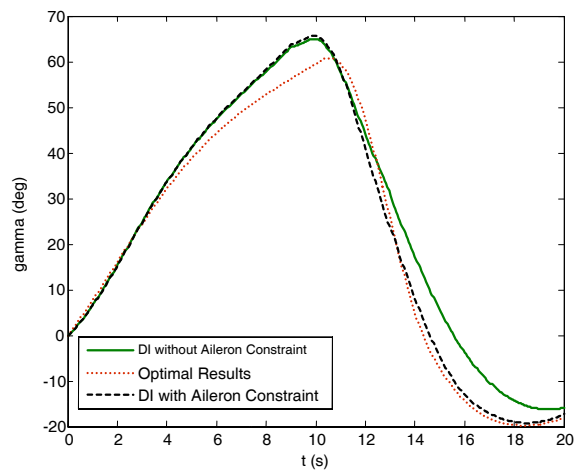

Fig. 7. Time variation of γ (deg)

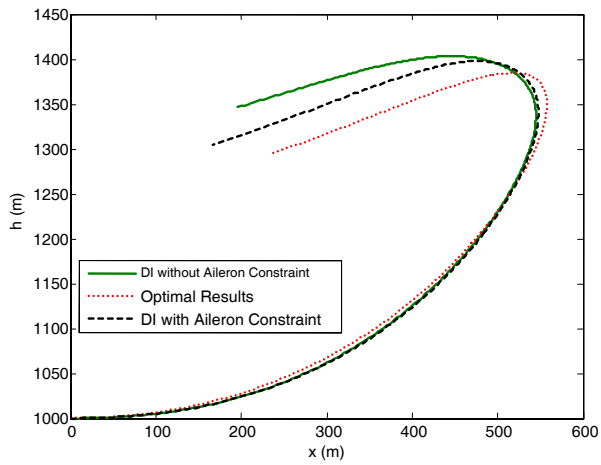

Fig. 8. variation of h versus x (m)

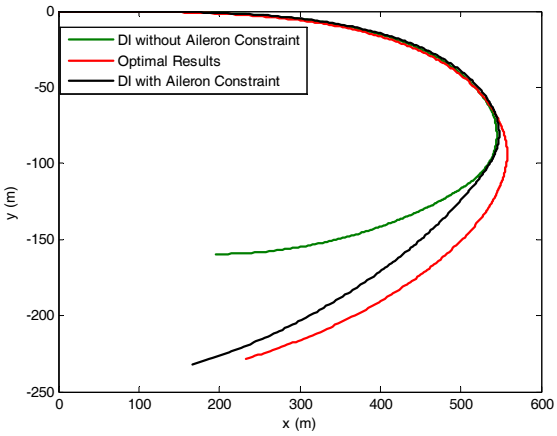

Fig. 9. variation of y versus x (m)

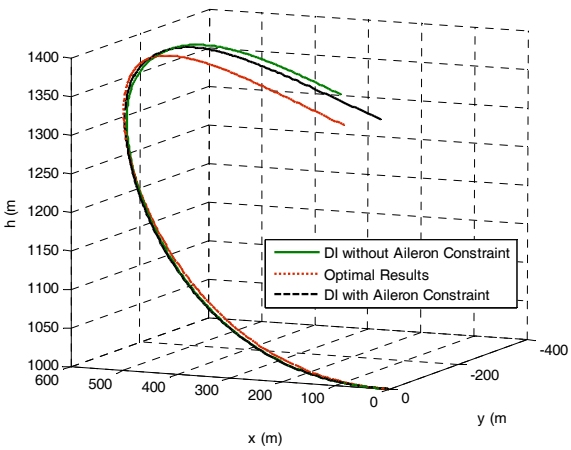

Fig. 10. Three-dimensional trajectory

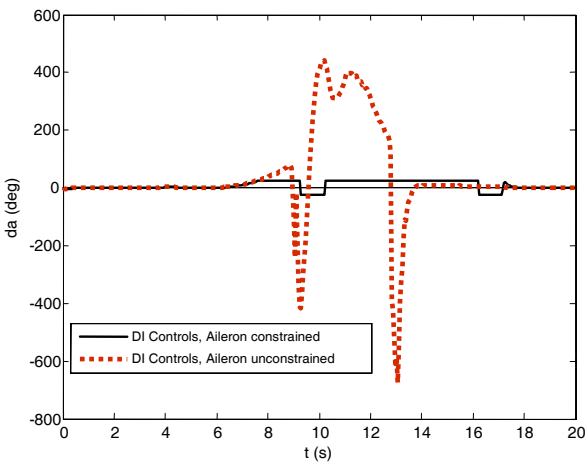

Fig. 11. Time variation of δ_a (deg)

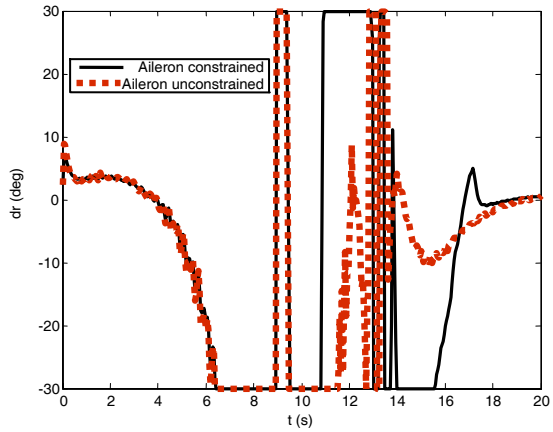

Fig. 12. Time variation of δ_r (deg)

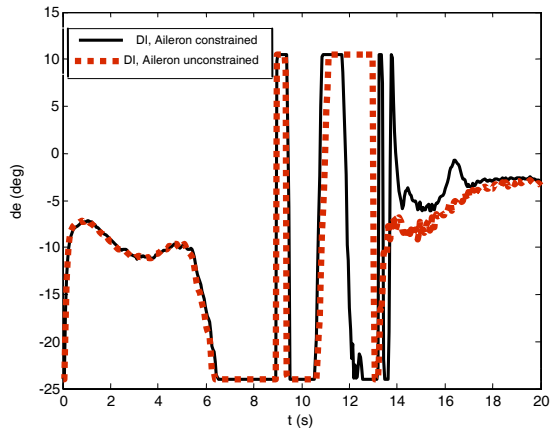

Fig. 13. Time variation of δ_e (deg)

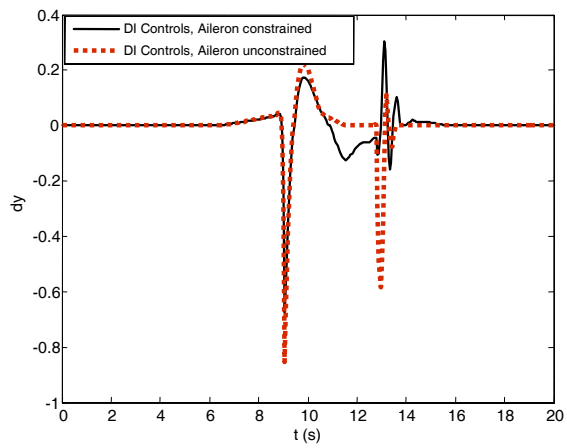

Fig. 14. Time variation of thrust deflection angle, δ_y, (deg)

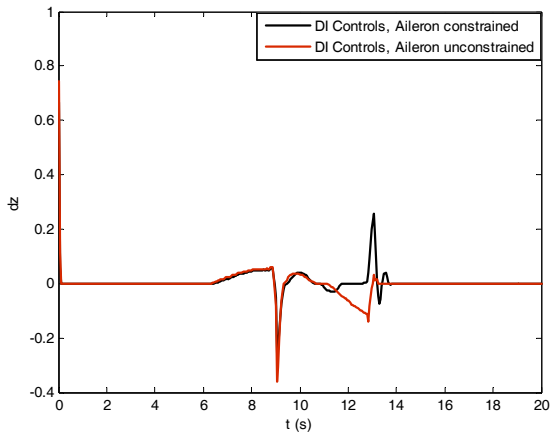

Fig. 15. Time variation of thrust deflection angle, δ_z, (deg)

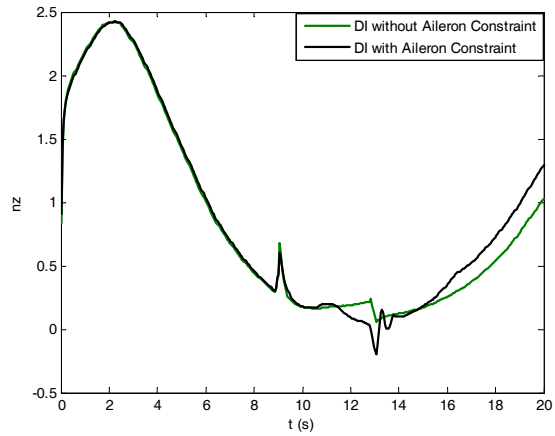

Fig. 16. Time variation of the load factor, n_Z

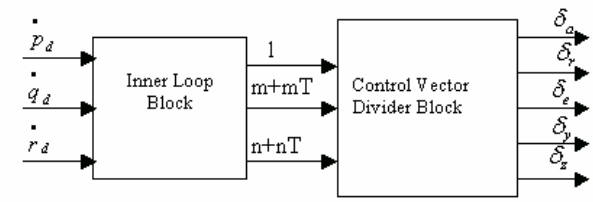

Fig. 17. Inner-loop configuration

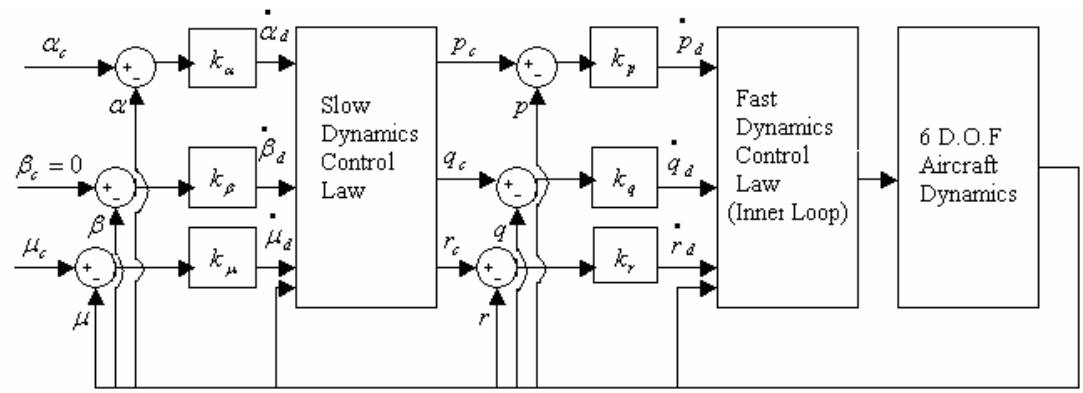

Fig. 18. Designed closed-loop control system